Journal of Electrical and Electronics Engineering Research Vol. 3(2), pp. 27-41, February 2011
Available online at http://www.academicjournals.org/jeeer
ISSN 2141-2367 ©2011 Academic Journals

Full Length Research Paper

Torque control in magnet flux estimation method of vector control with armature resistance estimation function of SPMSM using adaptive identification

Abdoulaye M'bemba Camara*, Yosuke Sakai and Hidehiko Sugimoto

Department of Electrical and Electronics Engineering, University of Fukui, Fukui 910-8507, Japan.

Accepted 7 February, 2011

In the conventional torque control (TC) of surface permanent magnet synchronous motor, the estimation of magnet flux becomes a big issue because the variation of permanent magnet flux that deteriorates the performance of torque controlled system. The injection molding machine contains a pressure control which is scarcely used on machine tools. The control of this pressure is very important for the operation of injection molding machine because, it depends on the permanent magnet flux which depends on the variations of temperature inside of the motor. With the increase of armature winding temperature, the permanent magnet temperature increases and the magnet flux decreases. Through that variation, the magnet flux is not treated constantly and then the magnet flux information becomes necessary to keep the pressure constant during the operation. Therefore, it is important to develop a fine force-control system. Generally, in force-control systems, the force information from the environment is detected by a force sensor. However, control systems using force sensors present problems related to signal noise, sensor cost, narrow bandwidth, and other factors. To overcome these problems, this paper proposes the estimation method of the magnet flux and the armature winding resistance based on the adaptive identification used in the SPMSM with the vector control in exchange of Force sensor (load cell). The success of the proposed method is showed by both of simulations and experiments.

Key words: SPMSM, torque control, magnet flux estimation method of vector control, armature resistance estimation, adaptive identification, mathematical model.

INTRODUCTION

In recent years, plastic has become the most widely used raw material in various fields. Plastic products are mainly manufactured using injection molding machines which uses surface permanent magnet flux synchronous motor. Many studies of electric injection molding machines have been carried out (Lu et al., 2001, 2007; Yang et al., 2007). The torque requires the control of amplitude of armature current and the same principle has been applied in interior permanent magnet synchronous motors. Recently, some noticeable attempts have been made to achieve wide speed ranges of constant-power operation with SPMSM motors using concentrated windings (El-Refaie and Jahns, 2005; El-Refaie et al., 2006). Large-scale production of plastic products requires high-performance position. However, the quality of plastic products depends on the injection force. For that reason, it is important to develop not only a high-performance position control system but also a fine force-control system. Regarding conventional force control, much research has been undertaken to develop force sensors to detect external force (Khayati et al., 2006; Takeda et al., 2007; Li et al., 2007). A typical injection molding machine senses the force information using a force sensor. However, highly sensitive force sensors are not economical. A typical force sensor has both initial and running costs. Moreover, force sensors confront problems such as noise and frequency bands.

In an ideal force-control system, force sensors should be attached to the same location as the actuator to realize an instantaneous force sensing process. However, in a conventional actual servo system, force sensors are mounted on different positions than the actuator.

*Corresponding author. E-mail: aziz71@u-fukui.ac.jp.

Consequently, it is difficult for force sensing systems to obtain force data accurately and instantaneously. To overcome these problems, many force-sensorless control methods have been proposed. Ohnishi et al. (1996) proposed the disturbance observer, which compensates the disturbance torque for the motor (Ohnishi et al., 1996). The disturbance observer estimates well the disturbance torque without a torque sensor. Ohishi et al. (2006) proposed a robust tracking servo system for the optical disk recording system. This system realizes a robust servo control using a force-sensorless method. Furthermore, the sensorless force-control method using the reaction torque observer has been applied (Murakami et al., 1993; Katsura et al., 2008; Tashiro et al., 2008). The reaction torque observer is based on the disturbance observer and friction model. This sensorless force-control method uses only the motor current information and motor position information. In other words, this torque estimation algorithm requires no additional sensor. A sensorless force control for an injection molding machine without any additional sensor has not been achieved yet.

The reaction torque observer is applied to the injection molding machine using a ball screw. The motion control system using the ball screw often has a resonant frequency (Zang et al., 2000; O'Sullivan et al., 2007). This torsional vibration affects the performance of reaction torque estimation (Ohba et al., 2008) and a reaction torque observer based on a two-inertia plant model considering the torsion phenomenon has been proposed (Ohba et al., 2009). These methods are inherent problem with the parameters variations due to the environnement effect. The method to estimate the magnet flux has been proposed (Camara et al., 2010) with robustness between magnet flux and armature winding resistance. But with the time, the armature winding resistance may affect the magnet flux. To overcome this problem, this paper proposed a flux estimation system with armature winding resistance function in order to control torque using adaptive identification without torque sensor controlling armature current with error less than 1%.

The stability is examined by bode diagram and the utility is confirmed by both of simulations and experiments.

MATERIALS AND METHODS

Mathematical model and linearization error equation of state

Composition of the proposed system

The voltages v_{da}, v_{qa} are given to a real SPMSM and mathematical model as an input. The Figure 1 shows estimated parameters $\hat{\phi}_{fa}$ $\hat{R}_a$ of mathematical model. This method expressed the torque reference current i_{qa}^* using the output of speed controller, the estimated magnet flux and armature winding resistance. Therefore, the estimated parameters are used in controller. The torque reference expression is showed in Equation 1:

$$\hat{T}_e = p\,\hat{\phi}_{fa}\,i_{qa} \quad \ldots\ldots\ldots\ldots\ldots\ldots\ldots\ldots\ldots\ldots\ldots\ldots\ldots\ (1)$$

$\hat{T}_e$ - estimated torque, p - number of pole pairs, $\hat{\phi}_{fa}$ - estimated magnet flux, i_{qa} - q axis current.

Mathematical model

The state equation of SPMSM in (d, q) coordinates is showed in Equation 2. Moreover, the Equation 3 shows the mathematical model .In Figure 1, the estimated current are described as $\hat{i}_{da}$, $\hat{i}_{qa}$ and estimated using $i_{da}, i_{qa}, v_{da}, v_{qa}, \hat{\phi}_{fa}, \hat{R}_a$:

$$\begin{bmatrix} L_a & 0 \\ 0 & L_a \end{bmatrix} \frac{d}{dt} \begin{bmatrix} i_{da} \\ i_{qa} \end{bmatrix} = \begin{bmatrix} -R_a & \omega L_a \\ -\omega L_a & -R_a \end{bmatrix} \begin{bmatrix} i_{da} \\ i_{qa} \end{bmatrix} + \begin{bmatrix} v_{da} \\ v_{qa} \end{bmatrix} - \omega_{re}\phi_{fa} \begin{bmatrix} 0 \\ 1 \end{bmatrix} \ldots\ldots\ldots\ (2)$$

$$\begin{bmatrix} L_a & 0 \\ 0 & L_a \end{bmatrix} \frac{d}{dt} \begin{bmatrix} \hat{i}_{da} \\ \hat{i}_{qa} \end{bmatrix} = \begin{bmatrix} -\hat{R}_a & \omega L_a \\ -\omega L_a & -\hat{R}_a \end{bmatrix} \begin{bmatrix} \hat{i}_{da} \\ \hat{i}_{qa} \end{bmatrix} + \begin{bmatrix} v_{da} \\ v_{qa} \end{bmatrix} - \omega_{re}\hat{\phi}_{fa} \begin{bmatrix} 0 \\ 1 \end{bmatrix} + \begin{bmatrix} g_{11} & g_{12} \\ g_{21} & g_{22} \end{bmatrix} \begin{bmatrix} i_{da} - \hat{i}_{da} \\ i_{qa} - \hat{i}_{qa} \end{bmatrix} \ldots\ldots \quad (3)$$

R_a : armature winding resistance L_a :d,q axes inductances, ϕ_{fa} permanent magnet flux,

v_{da}, v_{qa} :d,q axes voltages, i_{da}, i_{qa} :d,q axes currents, ω_{re} :synchronous angular frequency.

The current of the armature and the parameter with the sign ^ show "estimation" and the estimated parameter of ϕ_{fa} , R_a .Moreover, $g_{11}, g_{12}, g_{21}, g_{22}$ are mathematical model gains.

Linearization of estimation error of state equation

To apply linear system theory to controller design, the governing equations must be linearized. The estimation error of state equation is obtained by multiplying matrix inverse of inductance matrix to each side of the Equations 2 and 3:

$$\frac{d}{dt} \begin{bmatrix} i_{da} - \hat{i}_{da} \\ i_{qa} - \hat{i}_{qa} \end{bmatrix} = \begin{bmatrix} A_{11} & A_{12} \\ A_{21} & A_{22} \end{bmatrix} \begin{bmatrix} i_{da} - \hat{i}_{da} \\ i_{qa} - \hat{i}_{qa} \end{bmatrix} + \begin{bmatrix} B_{11} & B_{12} \\ B_{21} & B_{22} \end{bmatrix} \begin{bmatrix} \Delta\phi_{fa} \\ \Delta R_a \end{bmatrix} = Ae_{ia} + Bu \quad \ldots(4)$$

Where:

$$A_{11} = -\left(\hat{R}_a + g_{11}\right)/L_a, A_{12} = \left(\omega_{re}L_a - g_{12}\right)/L_a, A_{21} = \left(-\omega_{re}L_a + g_{21}\right)/L_a \quad A_{22} = -\left(\hat{R}_a + g_{22}\right)/L_a, B_{11} = 0, B_{12} = -i_{da}/L_a, B_{21} = -\omega_{re}/L_a, B_{22} = -i_{qa}/L_a$$

$$e_{ia} = \begin{bmatrix} i_{da} - \hat{i}_{da} \\ i_{qa} - \hat{i}_{qa} \end{bmatrix}, u = \begin{bmatrix} \Delta\phi_{fa} \\ \Delta R_a \end{bmatrix}$$

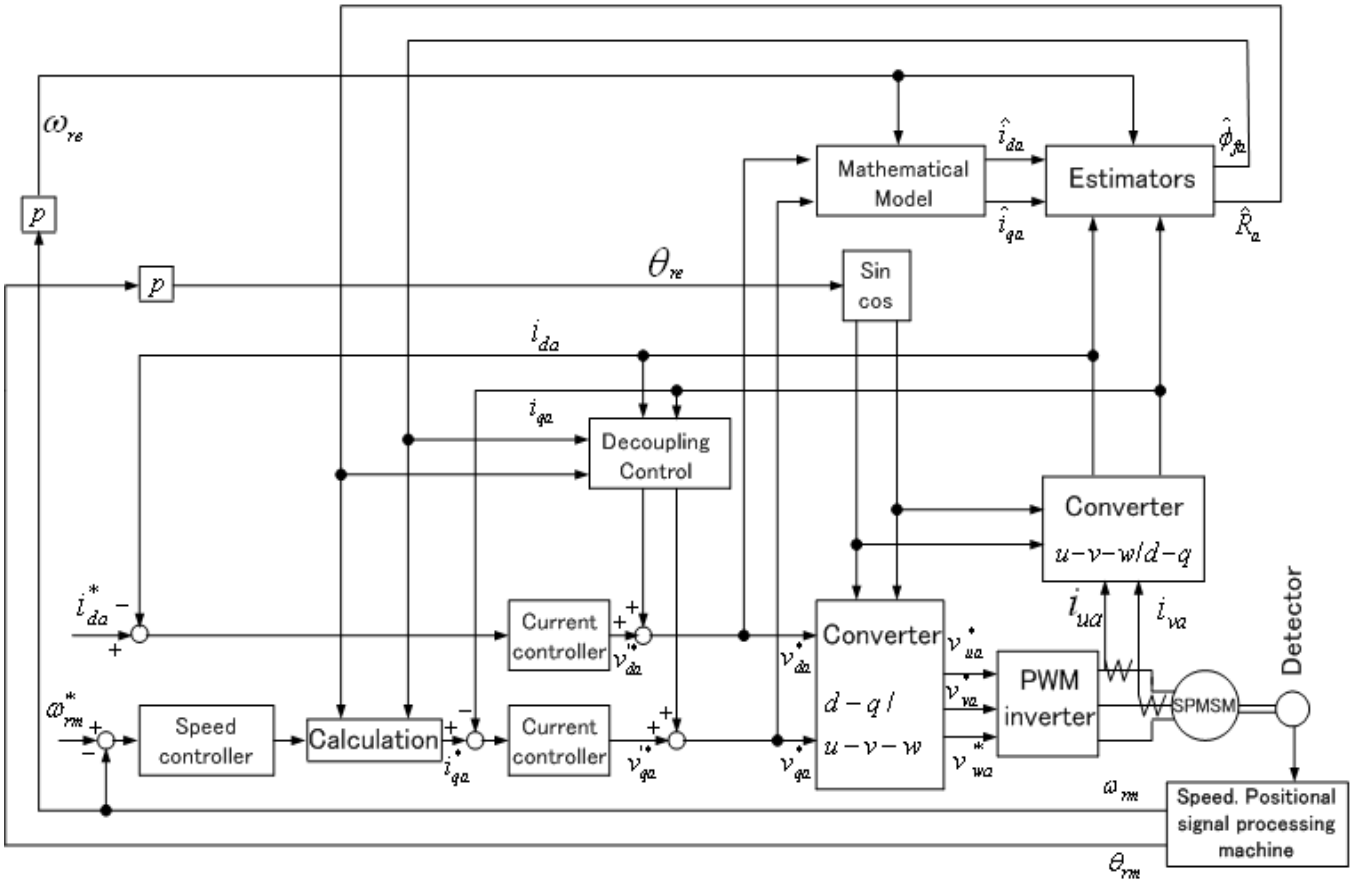

Figure 1. Block diagram of the control scheme.

The armature current, the armature voltage, the turning angle speed, and the armature winding resistance are expressed in the linear equation. The first separately equilibrium point and changes mathematical model gain when approximating. Each equilibrium point of the Equations 2 and 3 are assumed to be the same value.

$$s\begin{bmatrix} i_{da}-\hat{i}_{da} \\ i_{qa}-\hat{i}_{qa} \end{bmatrix}=\begin{bmatrix} A_{110} & A_{120} \\ A_{210} & A_{220} \end{bmatrix}\begin{bmatrix} i_{da}-\hat{i}_{da} \\ i_{qa}-\hat{i}_{qa} \end{bmatrix}+\begin{bmatrix} B_{110} & B_{120} \\ B_{210} & B_{220} \end{bmatrix}\begin{bmatrix} \Delta\phi_{fa} \\ \Delta R_a \end{bmatrix}=\mathrm{A_0 e_{ia}}+\mathrm{B_0 u} \quad \ldots \quad (5)$$

The mathematical model gain of Equation 6 is chosen:

$$g_{11}=g_{22}=g_a, g_{12}=\omega_{re}L_a, g_{21}=-\omega_{re}L_a \quad \ldots\ldots\ldots\ldots\ldots \quad (6)$$

The characteristic equation of the mathematical model is shown in Equation (7):

$$(sI-A_0)=\begin{bmatrix} s+\dfrac{\hat{R}_{a0}+g_{a0}}{L_a} & 0 \\ 0 & s+\dfrac{\hat{R}_{a0}+g_{a0}}{L_a} \end{bmatrix} \quad \ldots\ldots\ldots\ldots\ldots\ldots\ldots \quad (7)$$

The mathematical model gain g_a that Equation (7) comes to stabilize is chosen. Moreover, the linearization estimation error becomes as follows:

$$\begin{bmatrix} i_{da}-\hat{i}_{da} \\ i_{qa}-\hat{i}_{qa} \end{bmatrix}=(sI-A_0)^{-1}B_0\begin{bmatrix} \Delta\phi_{fa} \\ \Delta R_a \end{bmatrix}$$

$$=\begin{bmatrix} 0 & \dfrac{1}{s+\dfrac{\hat{R}_{a0}+g_{a0}}{L_a}}\left(\dfrac{i_{d\omega}}{L_a}\right) \\ \dfrac{1}{s+\dfrac{\hat{R}_{a0}+g_{a0}}{L_a}}\left(\dfrac{\omega_{fa0}}{L_a}\right) & \dfrac{1}{s+\dfrac{\hat{R}_{a0}+g_{a0}}{L_a}}\left(\dfrac{i_{q\omega}}{L_a}\right) \end{bmatrix}\begin{bmatrix} \Delta\phi_{fa} \\ \Delta R_a \end{bmatrix}$$

$$=P_0(s)\begin{bmatrix} \Delta\phi_{fa} \\ \Delta R_a \end{bmatrix} \quad \ldots\ldots\ldots\ldots\ldots\ldots\ldots\ldots\ldots \quad (8)$$

From where the transmission function matrix $P_0(s)$ is:

$$P_0(s)=\begin{bmatrix} 0 & \dfrac{1}{s+\dfrac{\hat{R}_{a0}+g_{a0}}{L_a}}\left(-\dfrac{i_{da0}}{L_a}\right) \\ \dfrac{1}{s+\dfrac{\hat{R}_{a0}+g_{a0}}{L_a}}\left(-\dfrac{\omega_{re0}}{L_a}\right) & \dfrac{1}{s+\dfrac{\hat{R}_{a0}+g_{a0}}{L_a}}\left(-\dfrac{i_{qa0}}{L_a}\right) \end{bmatrix} \quad \ldots\ldots\ldots\ldots\ldots \quad (9)$$

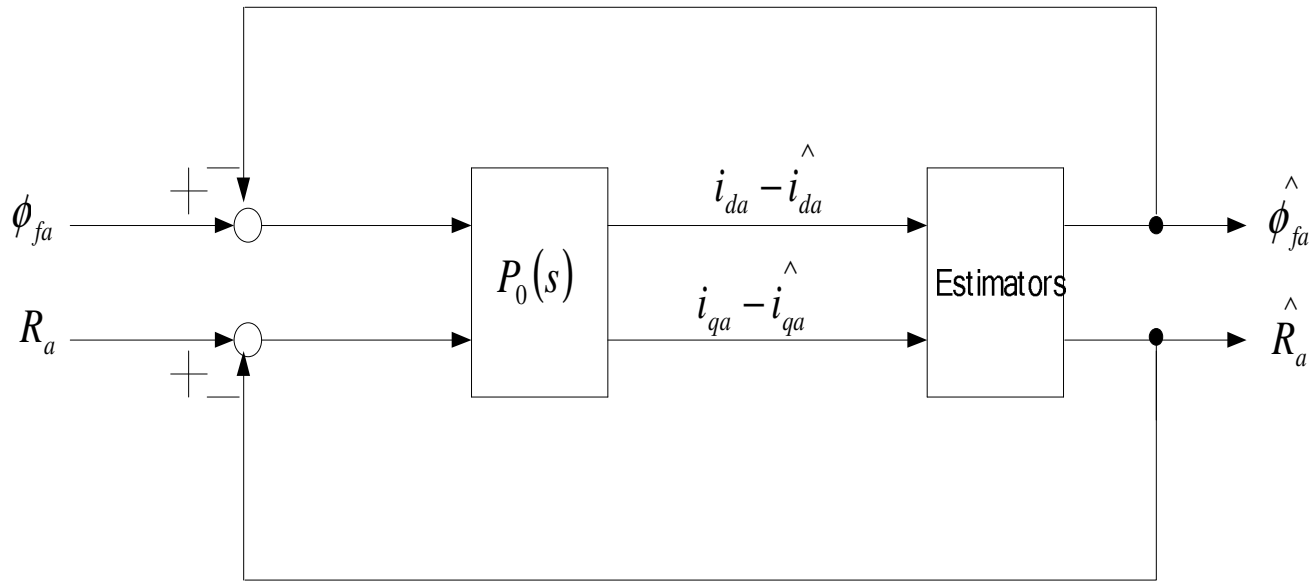

Figure 2. Construction of estimation system.

The inversion of $P_0(s)$ is:

$$P_0^{-1}(s) = \frac{\tilde{P}_0(s)}{\det(P_0)}$$

$$P_0^{-1}(s) = \begin{bmatrix} \left(s + \frac{\hat{R}_{a0} + g_{a0}}{L_a}\right)\left(\frac{L_a i_{qa0}}{\omega_{re0} i_{da0}}\right) & \left(s + \frac{\hat{R}_{a0} + g_{a0}}{L_a}\right)\left(-\frac{L_a}{\omega_{re0}}\right) \\ \left(s + \frac{\hat{R}_{a0} + g_{a0}}{L_a}\right)\left(-\frac{L_a}{i_{da0}}\right) & 0 \end{bmatrix} \quad \text{.....(10)}$$

COMPOSITION OF ESTIMATOR

Construction of estimation system

The Figure 2 shows the construction of estimation system with estimated parameters $\hat{\phi}_{fa}$ and $\hat{R}_a$.

$$\begin{bmatrix} \hat{\phi}_{fa} \\ \hat{R}_a \end{bmatrix} = P_0^{-1}(s) \begin{bmatrix} i_{da} - \hat{i}_{da} \\ i_{qa} - \hat{i}_{qa} \end{bmatrix} \quad \text{.....(11)}$$

And the estimator is:

$$\begin{bmatrix} \hat{\phi}_{fa} \\ \hat{R}_a \end{bmatrix} = \begin{bmatrix} \left(1 + \frac{1}{s}\frac{\hat{R}_a + g_a}{L_a}\right)\left(\frac{X_{p1} L_a i_{qa}}{\omega_{re} i_{da}}\right) & \left(1 + \frac{1}{s}\frac{\hat{R}_a + g_a}{L_a}\right)\left(-\frac{X_{p2} L_a}{\omega_{re}}\right) \\ \left(1 + \frac{1}{s}\frac{\hat{R}_a + g_a}{L_a}\right)\left(-\frac{X_{r1} L_a}{i_{da}}\right) & 0 \end{bmatrix} \begin{bmatrix} i_{da} - \hat{i}_{da} \\ i_{qa} - \hat{i}_{qa} \end{bmatrix} \quad \text{...(12)}$$

In the Equation 12, it is observed that ω_{re} and i_{da} exist in the denominator. This makes i_{da} as an important parameter because if it is zero, the magnet flux and armature winding resistance could not be estimated and hence, the experiment of this research is done at 5% of rated current ($i_{da} = 5\% \times I$). The same consequences will happen when the speed becomes zero, that is $\omega_{re} = 0$. Together Equations 8 and 12, we get:

$$\begin{bmatrix} \hat{\phi}_{fa} \\ \hat{R}_a \end{bmatrix} = \begin{bmatrix} \frac{X_{p20}}{s} & \frac{(-X_{p10} + X_{p20}) i_{qa0}}{\omega_{re0} s} \\ 0 & \frac{X_{r10}}{s} \end{bmatrix} \begin{bmatrix} \Delta\phi_{fa} \\ \Delta R_a \end{bmatrix} \quad \text{.....(13)}$$

Where X_{p10}, X_{p20} and X_{r10} represent each integrator gain.

In this paper, the magnet flux and armature winding resistance are estimated under the condition $X_{p10} \neq X_{p20}$. The Equation 2 can be used at speed near to zero and first of all, we need for the estimation of magnet flux to fill the condition that the speeds rotate faster than resolution.

Figure 3 shows the characteristic of the stability. The gain and phase differences between the input and output of the estimation system are a simple pole. From the Figure 3, it is understood that, less than 1 rad/sec, the gain is nearly 0dB and also the phase is 0deg which express that the variation of R_a is slow. Therefore, the possibility of estimation of R_a is expressed according to Figures 4.

Improvement of the speed resolution

The calculation of the improvement of the speed resolution is

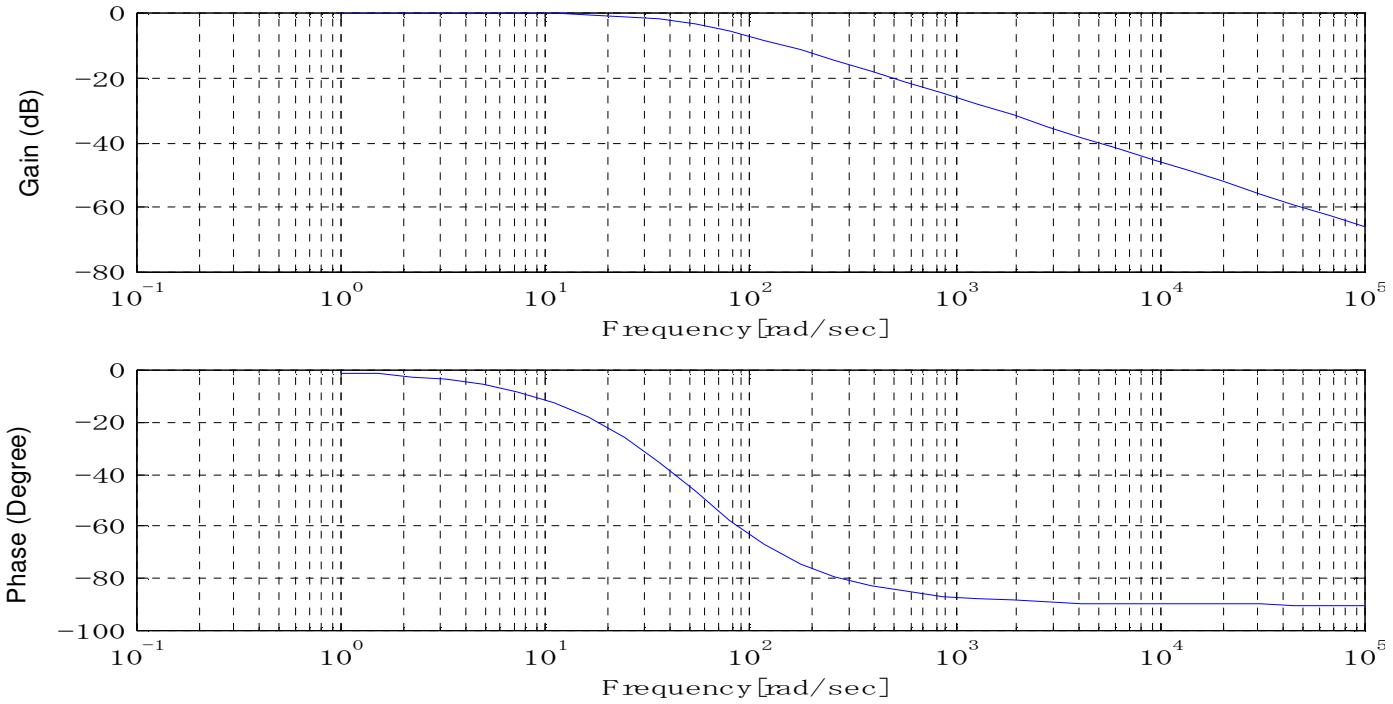

Figure 3. Bode diagram of $\hat{\phi}_{fa} / \phi_{fa}$.

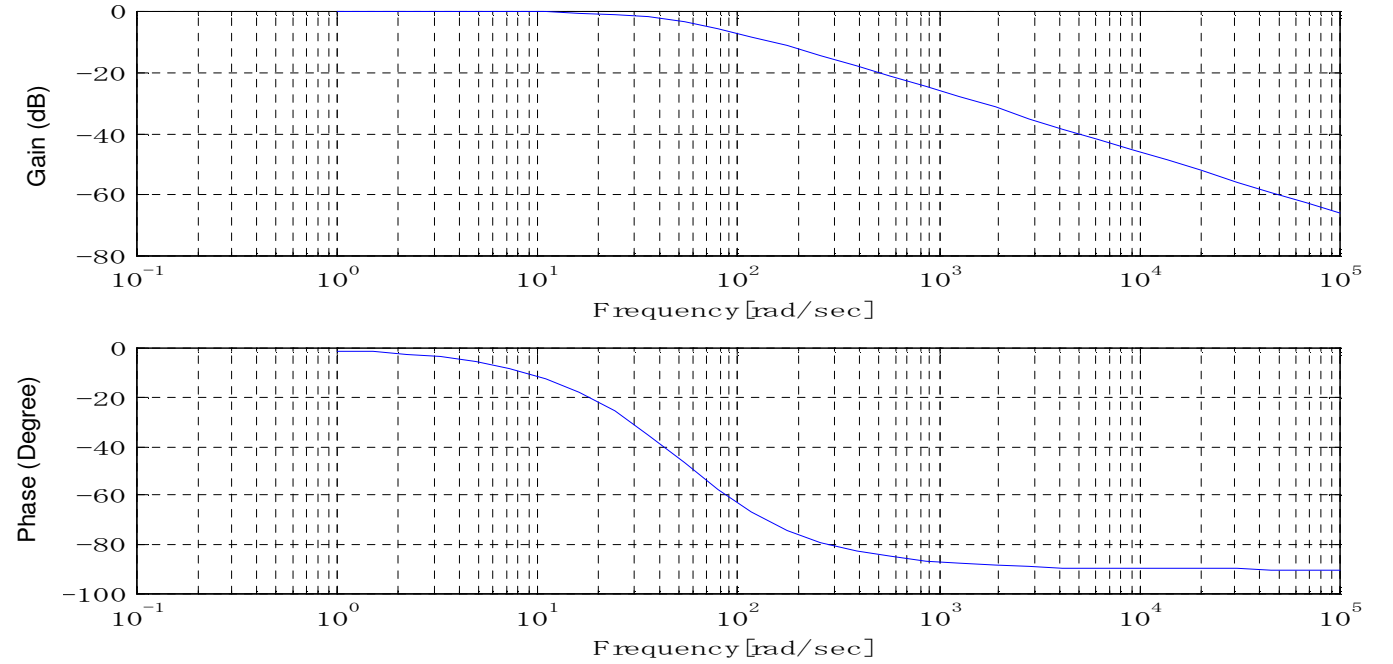

Figure 4. Bode diagram of $\hat{R}_a / R_a$.

recorded as follows. Speed resolution $\Delta \omega_{rm}$ (mechanical speed) is recorded as follows:

$$\Delta \omega_{rm} = \frac{2\pi}{n_p \bullet t_c \bullet N} [\text{rad} / \text{sec}] \quad \text{.....} \quad (14)$$

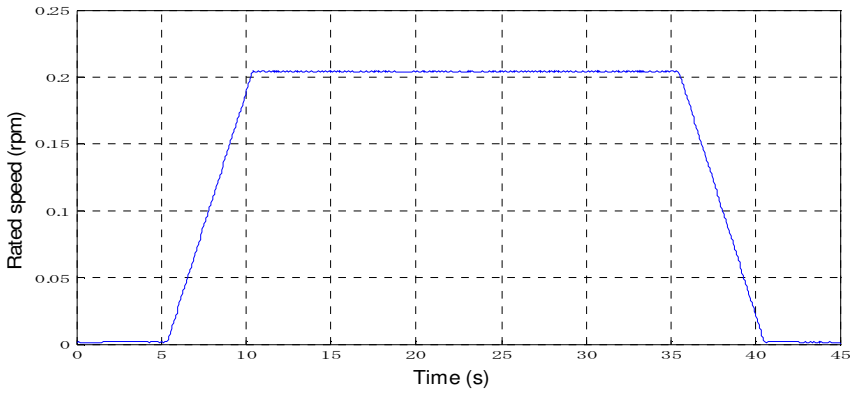

Figure 5. The rated speed improvement.

Table 1. Rating of tested motor.

Rated power		1.5kW
Rated current		8.6 A
Rated speed		1000rpm
Number of pole-pairs	p	3
Torque Constant	ϕ_{fa}	0.1946Wb
Armature winding resistance	R_a	$0.5157\,\Omega$
Armature winding self-inductance	L_a	2.452mH
Moment of inertia	J	$0.00525\,kg \cdot m^2$

Here $n_p\,[\text{pulse/rev}\ ]$: the encoder pulse number $t_c\,[\mu\text{sec}]$: operational period, N number of moving average samples. $n_p = 4000\,[\text{pulse/rev}\ ], t_c = 204.8\,[\mu\text{sec}\ ], N = 64$.

The Equation 14 shows the improvement of the speed resolution with an increase in the number of samples of moving averages. That is necessary because even at speed near to zero, we can detect the speed, and the flux and armature winding resistance estimation becomes possible and the Figure 5 shows the improvement of the speed resolution during the experiment.

SIMULATION AND EXPERIMENTAL CONDITIONS

Simulation

The estimation of magnet flux is simulated by using Matlab/Simulink. This time, when the proposed magnet flux estimation method was simulated, the PWM inverter was omitted.

Experimental condition

A test system was composed of a Digital Signal Processor DSP (TMS320C31-5kHz) control system (Texas instruments), a 3-phase PWM inverter and a 1.5 kW SPMSM. The operation cycle is 200 μs , the career frequency of the PWM inverter that drove the evaluation machine was assumed to be 5 KHz. The torque dectector is used for the measure of torque. The detected current and voltage are fed to the input of DSP and then calculates the voltage order. The voltage instruction from DSP is converted into the PWM signal and then the short-circuit prevention time is added by FPGA which generates output to the circuit of the drive at the gate. Signal carrier's (triangular wave) cycle was assumed to be 204.8 μs using the triangular wave comparison method for the generation of the PWM signal. Hall CT (HAS-50S: LEM) was used for the current detector. The voltage proportional to the current from hall CT is output, and the voltage signal is converted into the digital signal with 16 bit A/D converter (AD976:AnalogDevices). DC power voltage E_{DC} of the inverter is detected with 12 bit A/D converter (AD7864: Analog Devices) connected through the partial pressure machine.

Voltage type PWM inverter is composed of the power-module and the circuit of the drive at the gate. IGBT-IPM (6MBP30RH060: Fuji Electric Co., Ltd.) was used for the power-module. The direct current voltage power supply of the inverter has vector control of faction 2.2 kW of the three-phase circuit 200 V type inverter (FRN2.2VG7S-2: Fuji Electric Co., Ltd.) that controls the torque and DC linked the load machines. The pulse number output from the encoder used this time is 1000 pulses a rotation. As for the voltage detection error margin $\pm 1/\left(2^{13}\right) = \pm 1/8192$, the delay of the voltage feed back
loop becomes $300\ \mu s$, which is 1.5 times at sampling period $204.8\mu s$.

Table 1 shows the constants of SPMSM for the simulation and the experiment. As for injection molding machine, the torque is particularly important specially at low speed and the estimation of the magnet flux at low speed become necessary. The condition of the simulation is with the increase of the armature winding temperature, the armature winding resistance increases and the magnet flux decreases as showed in the Figures 6 and 7.

The simulation omitted the PWM inverter and because of the space, all the results of simulation and experiment are not showed in this paper.

RESULTS

In this simulation, during 50 s, the variation of the magnet

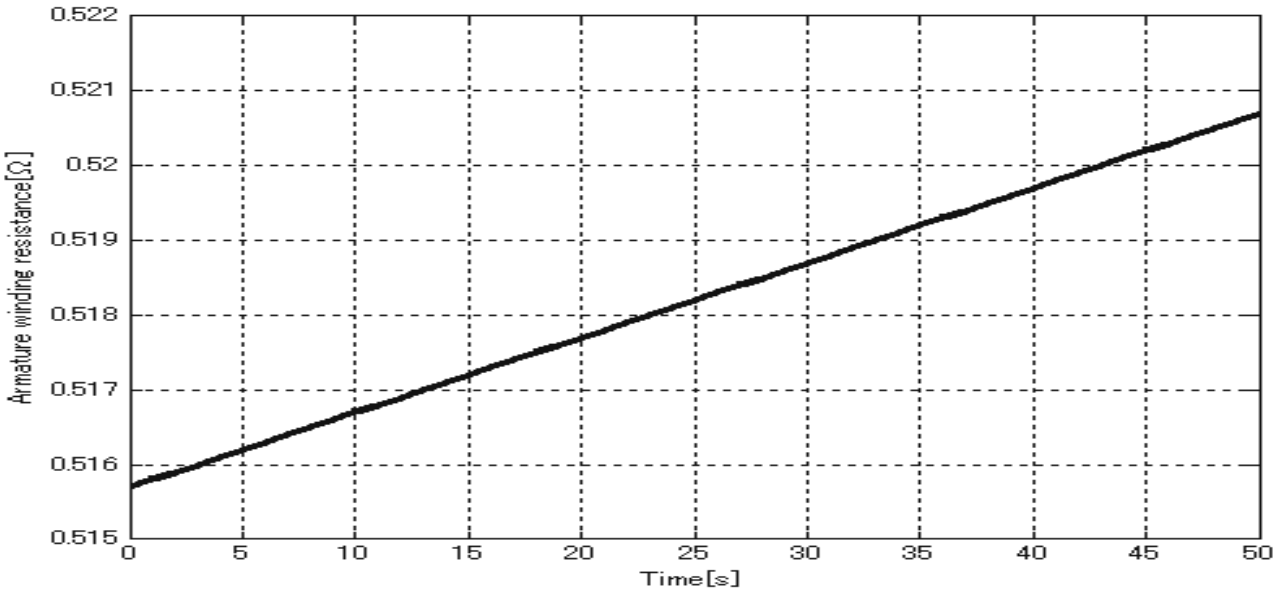

Figure 6. Simulation conditions for armature winding resistance variations.

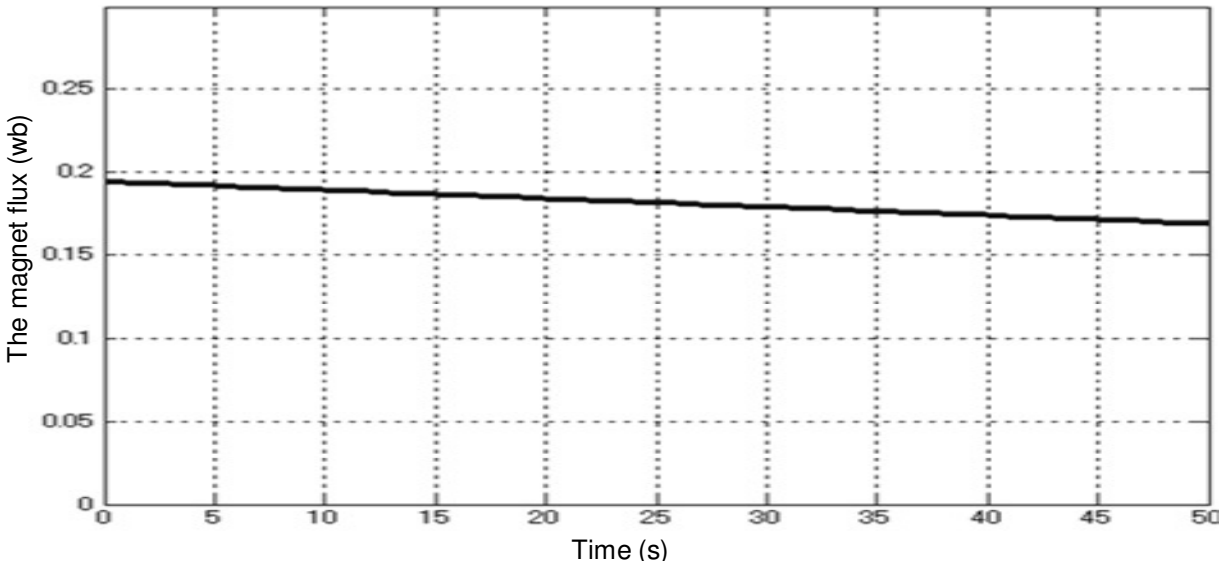

Figure 7. Simulation conditions for the magnet flux variations.

flux and the armature resistance of SPMSM can be observed with the increase of the temperature, although, in real machine during the same period the temperature would not increase to lead the such variation of magnet flux and armature resistance of SPMSM but because of the stability of the simulation, this research would not have the negative effect in the real machine.

The simulation results in Figures 6 and 7 shows that when the temperature increase, the armature winding resistance increase and then the magnet flux decrease consequently. Figure 8 shows the simulation result of estimated armature winding resistance and expressed its performance. Figures 9, 10 and 11 showed the simulation results of estimated flux at low speed with no-load; 50 and 100% load. The initial value is fixed at 0,295 Wb and the estimation started at 0.8 s.

Figures 12, 13 and 14 showed the simulation results of estimated flux at high speed with no-load; 50 and 100% load.

The experiment results of estimation flux at low speed showed in Figures 15, 16 and 17 with no-load, 50 and100% load. The experiment is realized in the same

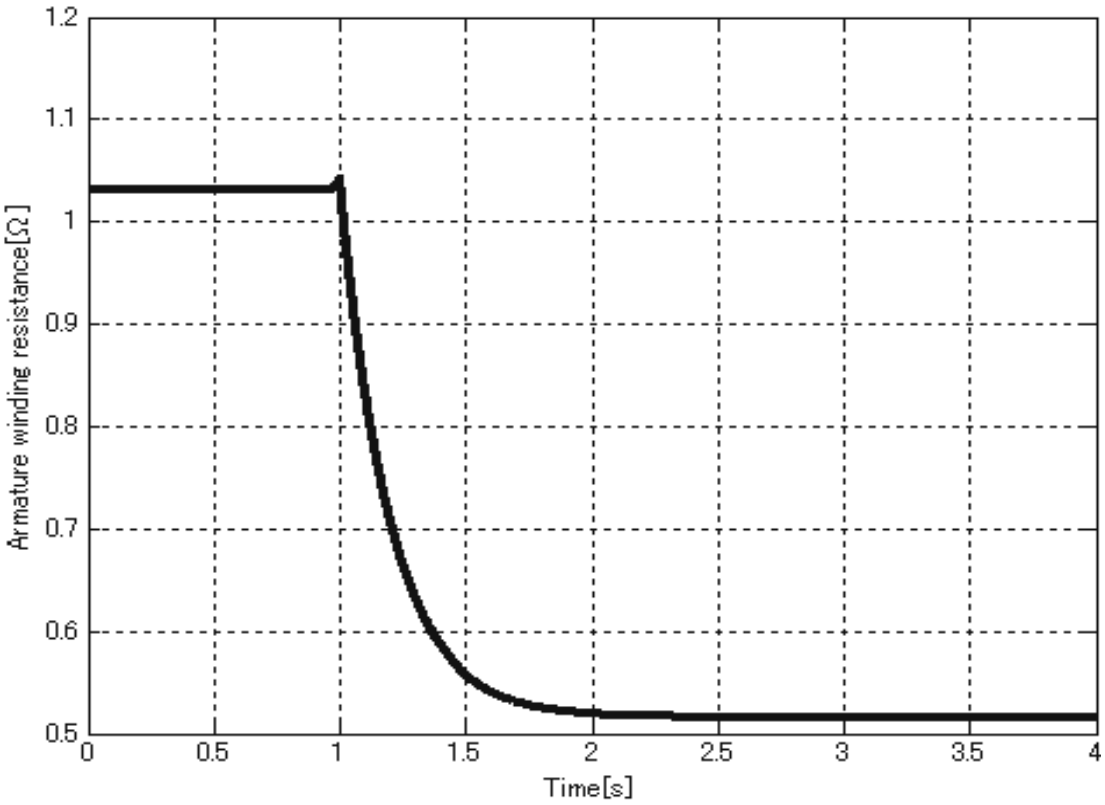

Figure 8. Simulation result of estimated armature winding resistance.

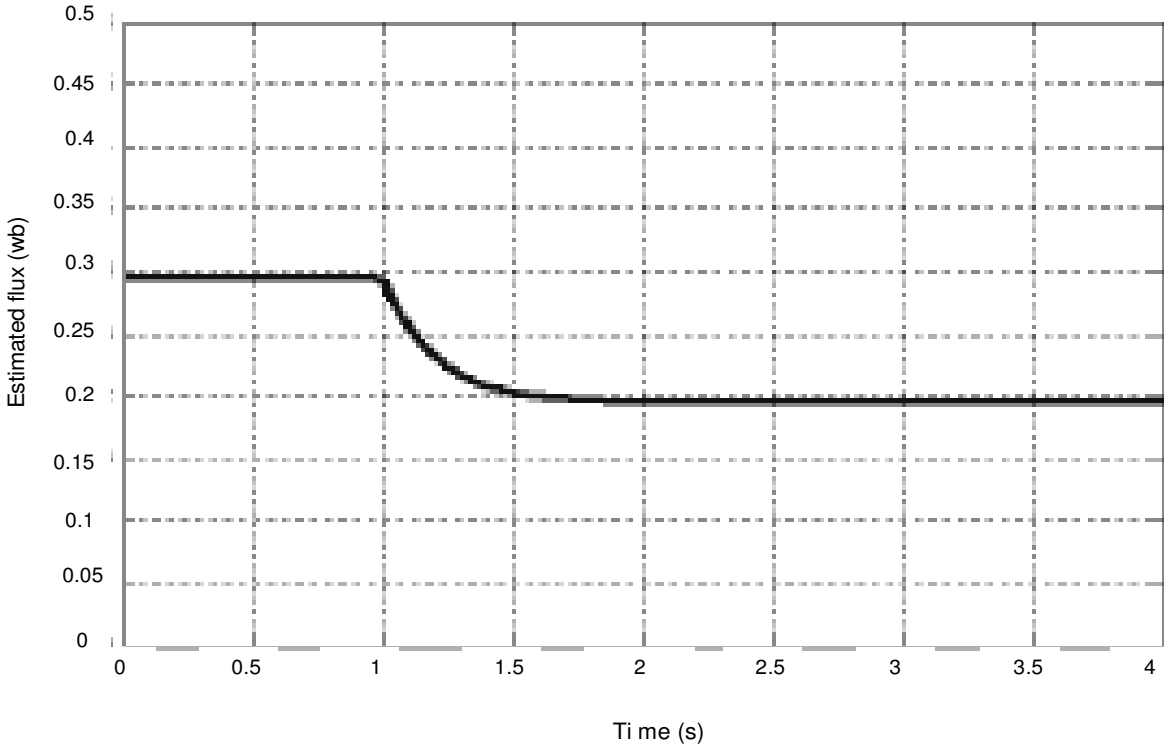

Figure 9. Simulation result of estimated magnet flux (no-load, 10 rpm).

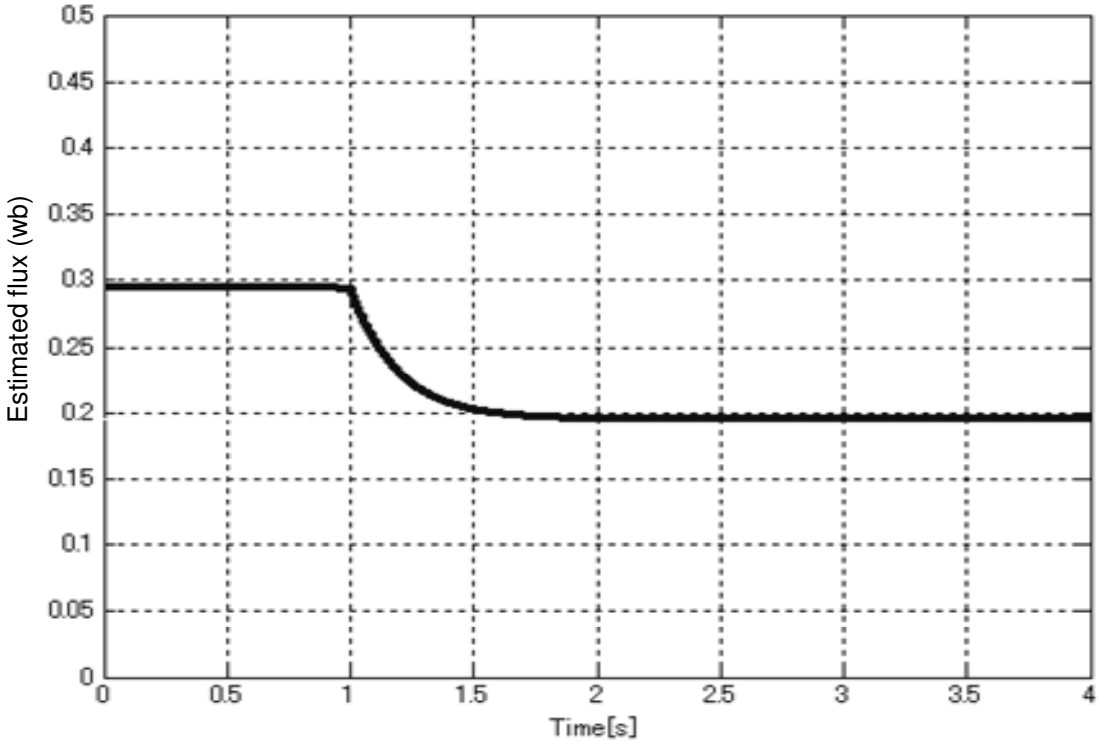

Figure 10. Simulation result of estimated magnet flux (50% load, 10 rpm).

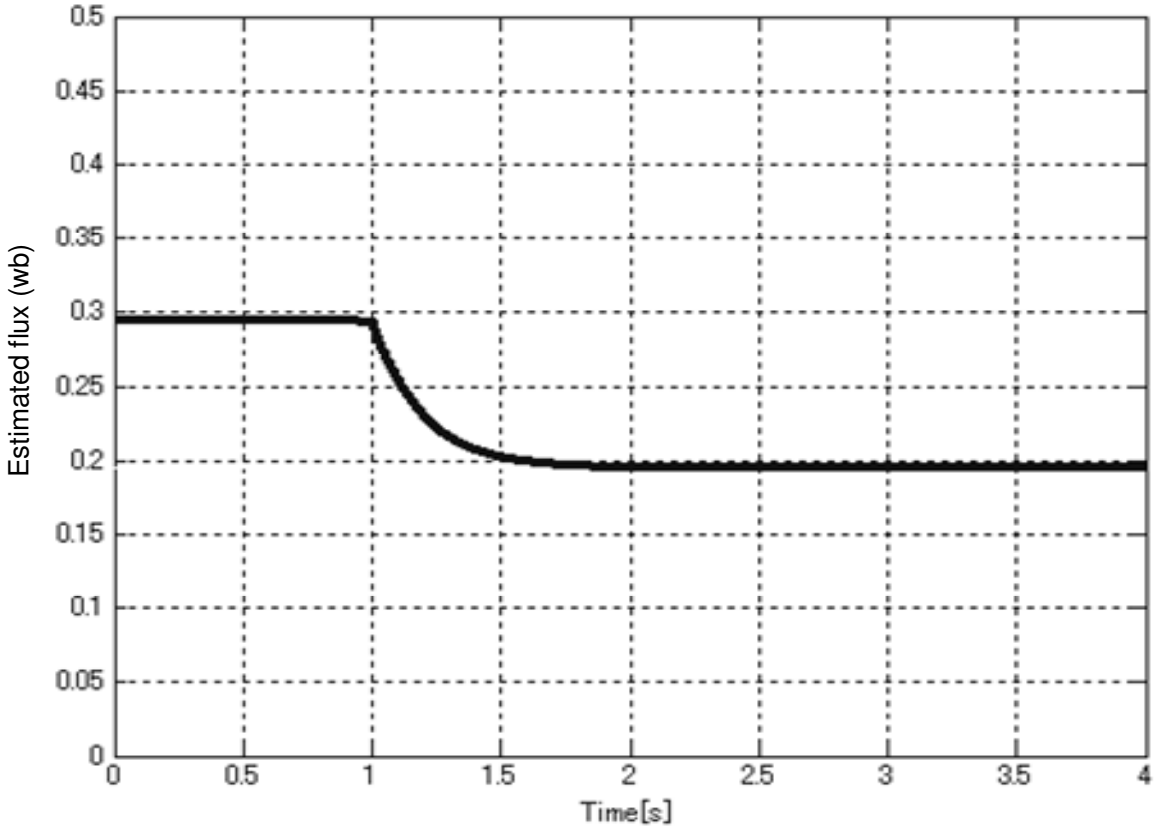

Figure 11. Simulation result of estimated magnet flux (100%load, 10rpm).

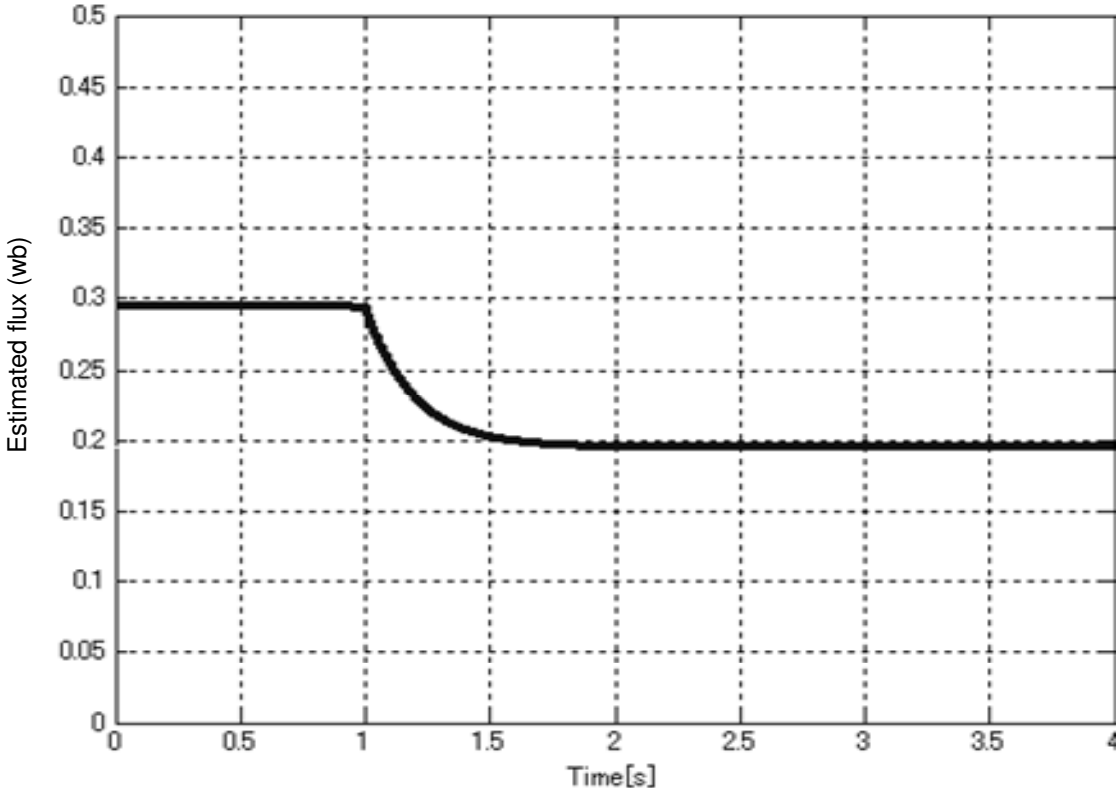

Figure 12. Simulation result of estimated magnet flux (no-load, 1000rpm).

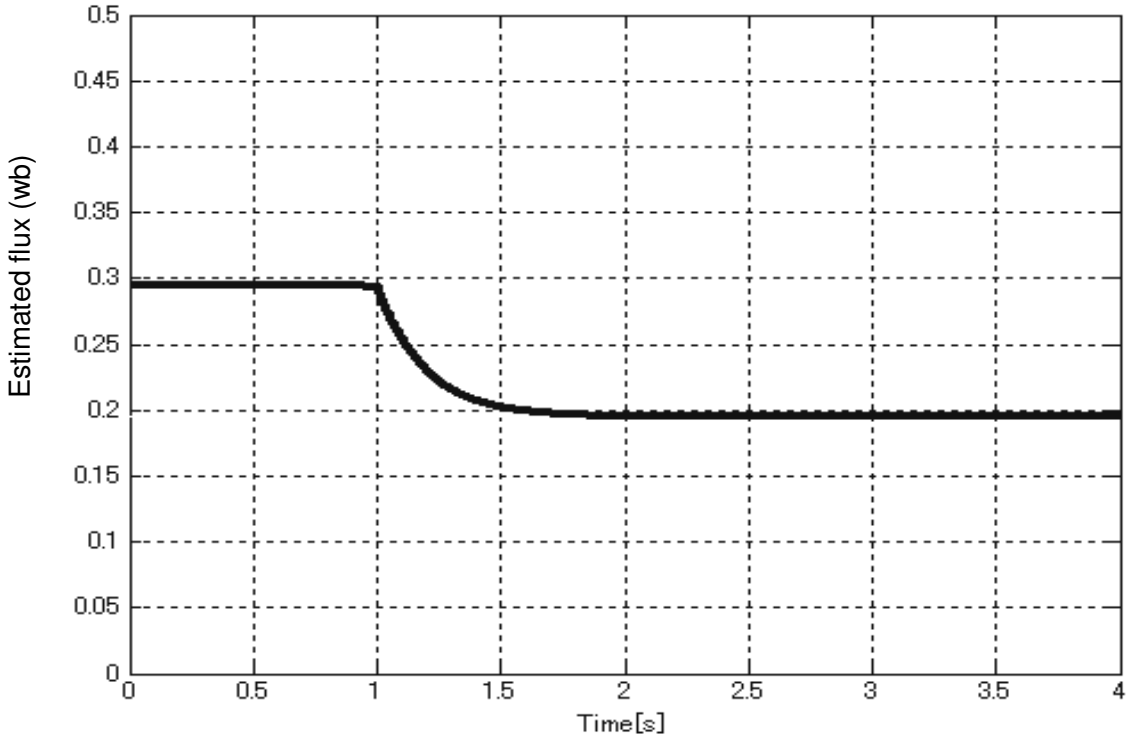

Figure 13. Simulation result of estimated magnet flux (50%load, 1000rpm).

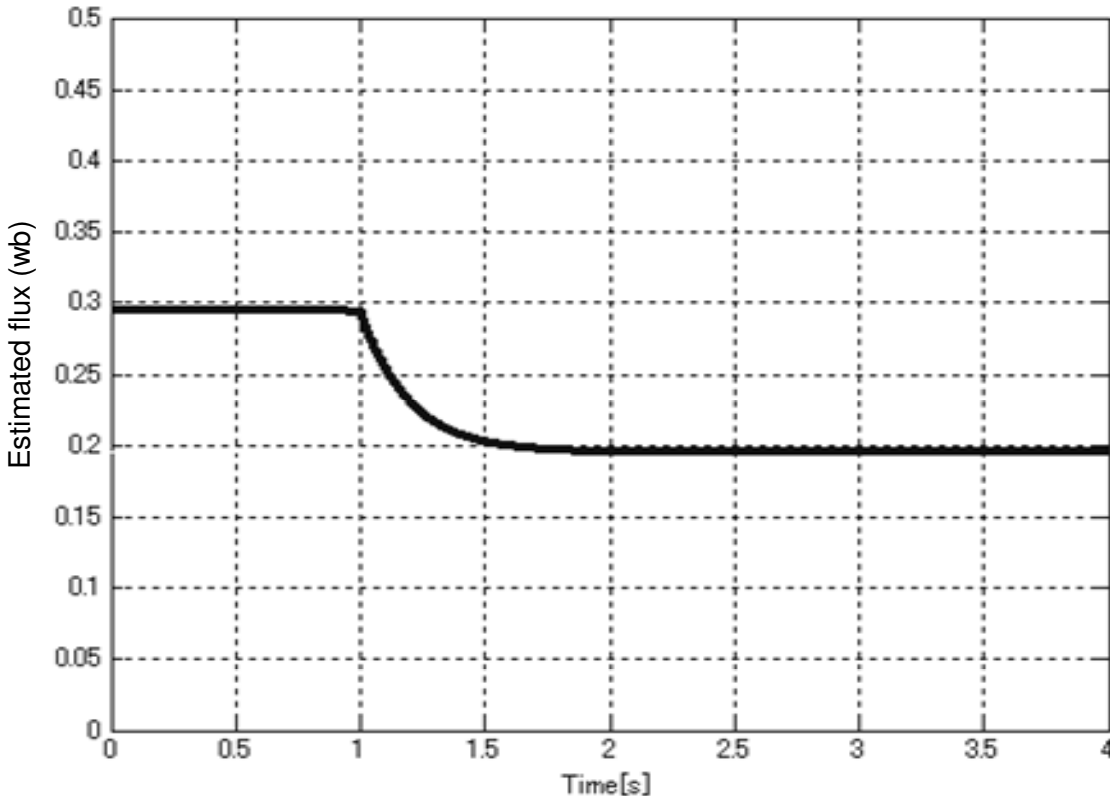

Figure 14. Simulation result of estimated magnet flux (100%load, 1000rpm).

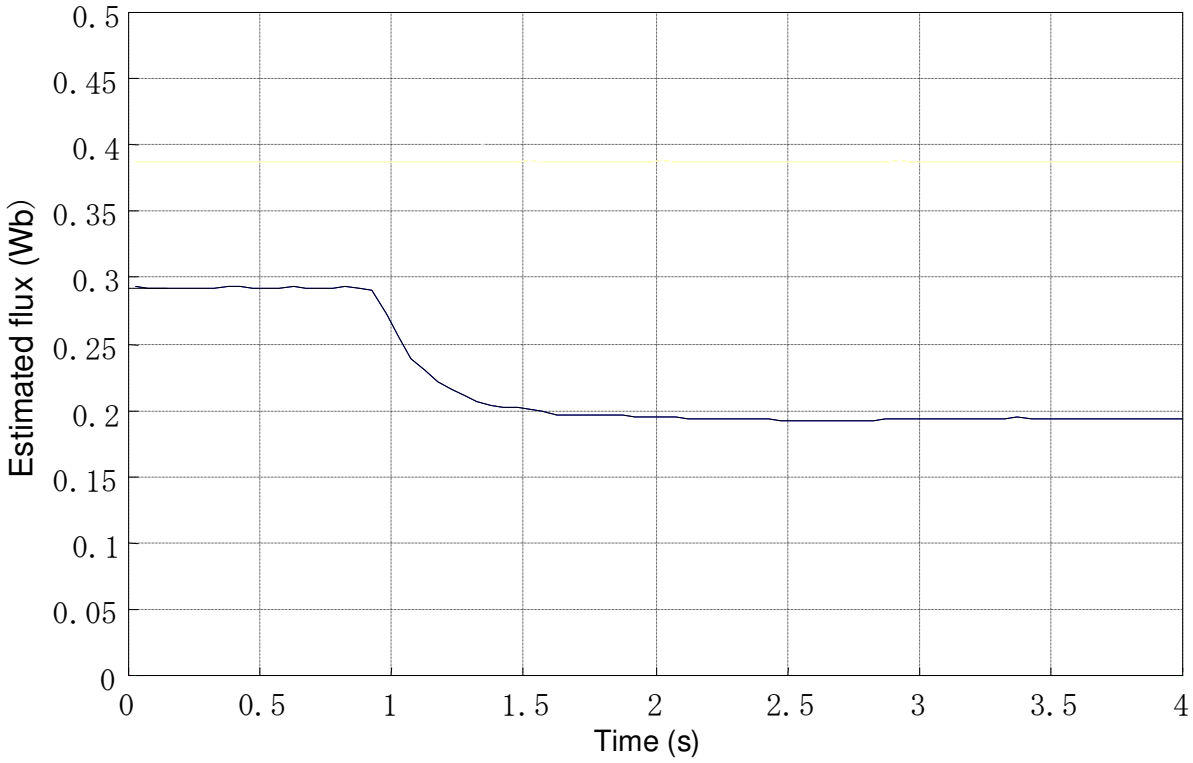

Figure 15. Experimental results of estimated magnet flux (No-load, 20 rpm).

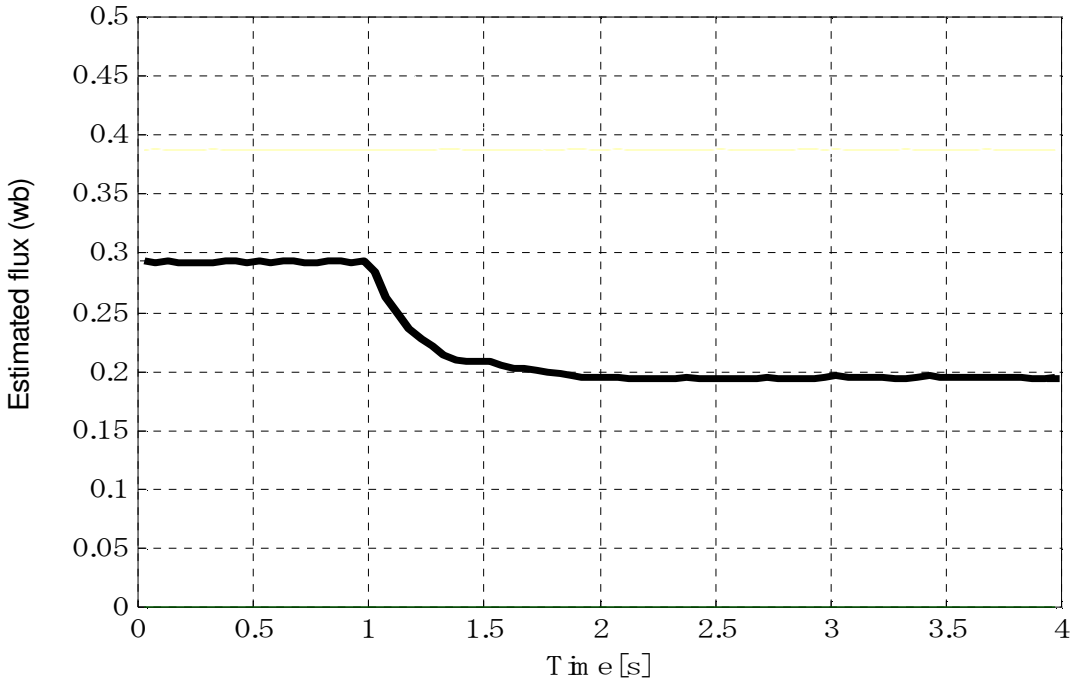

Figure 16. Experimental results of estimated magnet flux (50% load, 20 rpm).

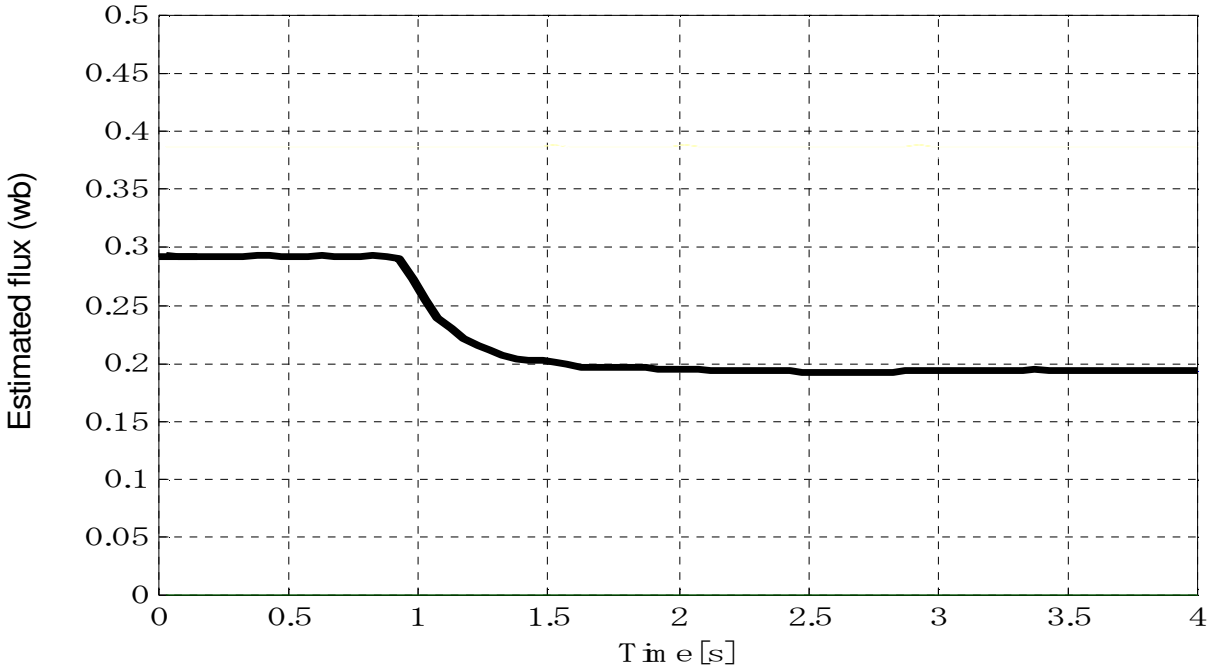

Figure 17. Experimental results of estimated magnet flux (100% load, 20 rpm).

condition with the simulation.

This experiment shows that, the estimation of magnet flux was effective because the voltage sensor is used in the experimental operation and hence the estimation error is 0.3% less than 0.5%. Also, this results showed the performance of experiment compare to the results of simulation at the same condition. Figures 18, 19 and 20 showed the simulation results of estimated flux at high

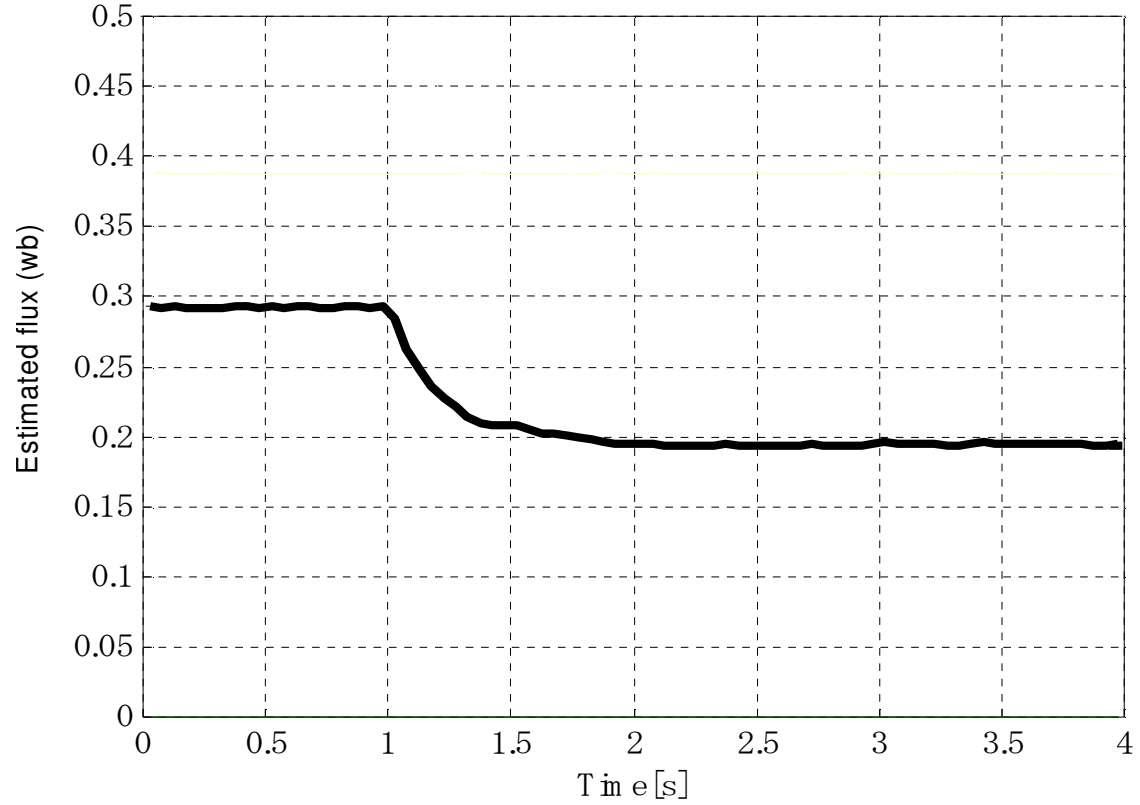

Figure 18. Experimental results of estimated magnet flux (No-load, 1000 rpm).

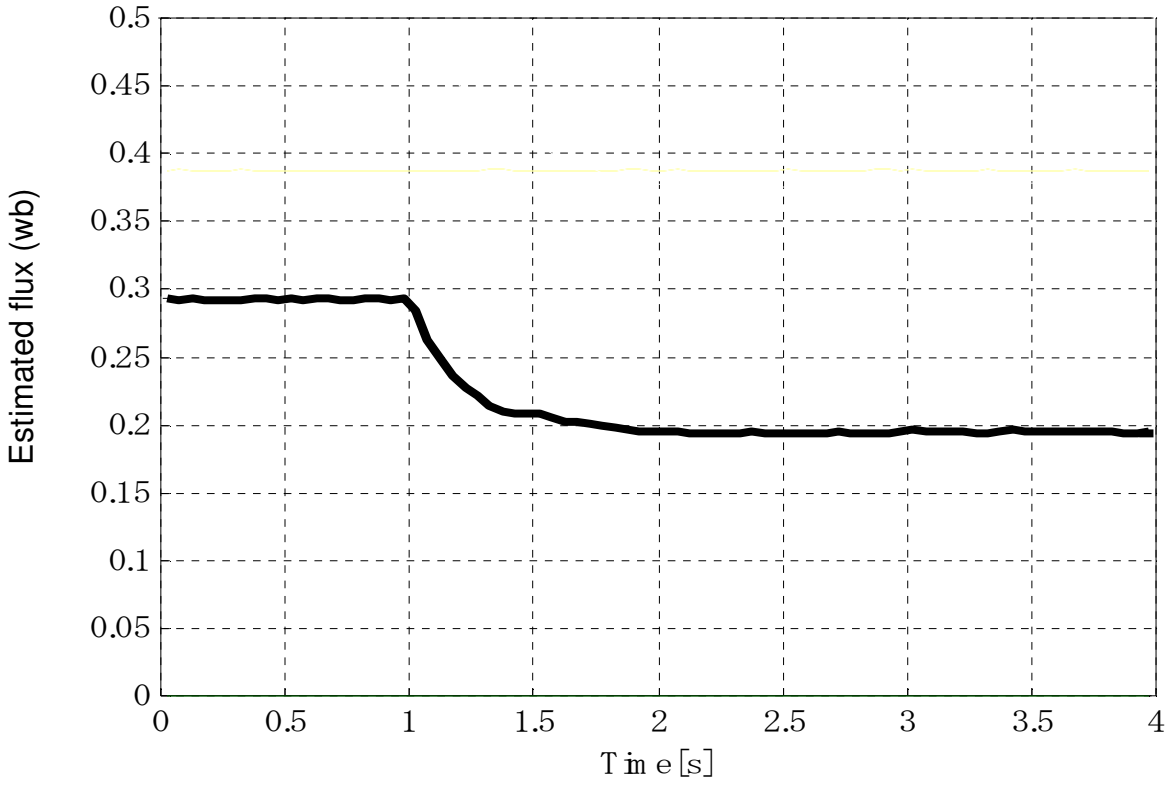

Figure 19. Experimental results of estimated magnet flux (50% load, 1000 rpm).

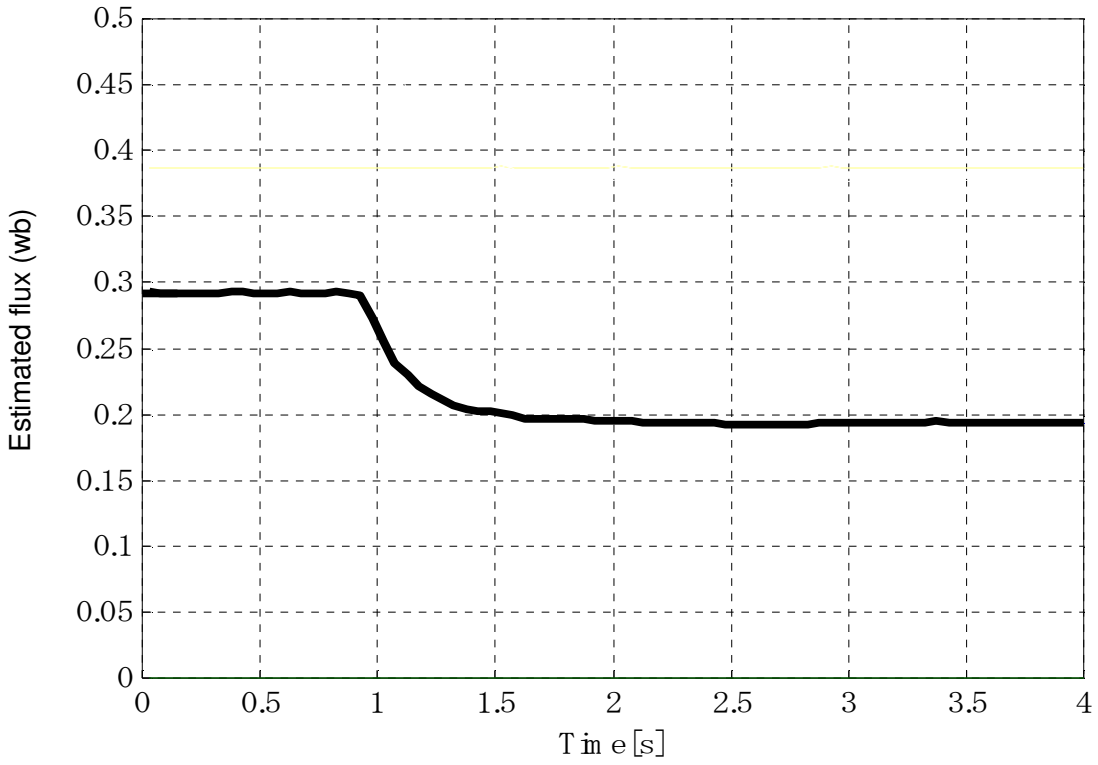

Figure 20. Experimental results of estimated magnet flux (100% load, 1000 rpm).

speed with no-load; 50%load and 100%load respectively.

DISCUSSION

The magnet flux information is important for controlling the torque of the SPMSM with vector control. The existing methods are based on a model torque control system using a torque observer but all these methods have some Inherent problems with the parameters variations due to the environment effect.

The authors propose in this work a method for estimating the magnet flux and armature winding resistance of the SPMSM with vector control using adaptive identification. The proposed method showed good estimated performance by designing and simulating the estimator of the magnet flux from linearization error state equation. This study presents magnet flux estimation system in order to control torque without torque sensor controlling armature current with robustness to the parameters variations due to the environment.

Conclusion

The magnet flux and armature winding resistance information's are important for controlling the torque of the SPMSM with vector control of the injection molding machine during the operation to be constant even at low speed. The authors propose in this work a new method for estimating the magnet flux of the SPMSM with vector control. The proposed method showed good estimated performance by designing and simulating the estimator of the magnet flux and armature winding resistance from linearization error of state equation.

ACKNOWLEDGEMENTS

The authors sincerely acknowledge Professor Dr. HIDEAKI NIKI, Department of Power Nuclear for his sincere help.

REFERENCES

Camara AM, Sakai Y Sugimoto H (2010). Permanent magnet flux estimation method of vector control SPMSPM using adaptive idenfication. J. Electrical Electronics Eng. Res., 2(4): 85-94.

El-Refaie AM, Jahns TM (2005). Optimal flux weakening in surface PM machines using fractional-slot concentrated windings. IEEE Trans. Ind., 41(3): 790-800.

El-Refaie AM, Jahns TM, McCleer PJ, McKeever JW (2006), Experimental verification of optimal flux weakening in surface PM machines using concentrated windings. IEEE Trans. Ind., 42(2): 443-453.

Katsura S, Irie K, Ohishi K (2008).Wideband force control by position acceleration integrated disturbance observer. IEEE Trans. Ind. Electron., 55(4): 1699-1706

Khayati K, Bigras P, Dessaint LA (2006). A multistage position/force

control for constrained robotic systems with friction: Joint-space decomposition, linearization, and multiobjective observer/controller synthesis using LMI formalism. IEEE. Trans. Ind. Electron., 53(5): 1698-1712.

Lu CH, Tsai CC, Liu CM, Chang YH (2007). Predictive control based on recurrent neural network and application to plastic injection molding processes.In Proc. IEEE IECON, pp. 792-797.

Lu CH, Tsai CC (2001). Adaptive decoupling predictive temperature control for an extrusion barrel in a plastic injection molding process. IEEE Trans. Ind. Electron., 53(5): 968-975.

Murakami T, Yu F, Ohnishi K (1993).Torque sensorless control in multidegree-of-freedom manipulator.IEEE Trans. Ind. Electron., 40(2): 259-265.

Ohba Y, Ohishi K, Katsura S, Yoshizawa Y, Kageyama K, Majima K (2008). Sensor-less force control for injection molding machine using reaction torque observer. in Proc.IEEE ICIT, Chengdu, China, pp. 1-6.

Ohba Y, Ohishi K, Katsura S, Yoshizawa Y, Kageyama K, Majima K (2009). Sensor-less force control for injection molding machine using reaction torque observer considering torsion phenomenon. in *Proc.* IEEE Trans. Inds. Electron., 56(8): 2955-2960.

Ohishi K, Miyazaki T, Inomata K, Yanagisawa H, Koide D, Tokumaru H (2006).Robust tracking servo system considering force disturbance for the optical disk recording system. IEEE Trans. Ind. Electron., 53(3): 838-847

Ohnishi K, Shibata M, Murakami T (1996).Motion control for advanced mechatronics. IEEE/ASME Trans. Mechatronics,1(1): 56-67

O'Sullivan TM, Bingham CM, Schofield N (2007).Observer-based tuning of two-inertia servo-drive systems with integrated SAW torque transducers. IEEE Trans. Ind. Electron., 54(2): 1080-109.

Takeda T, Hirata Y, Kosuge K (2007).Dance step estimation method based on HMM for dance partner robot. IEEE Trans. Ind. Electron., 54(2): 699-706.

Tashiro S, Murakami T (2008).Step passage control of a power-assisted wheelchair for a caregiver.IEEE Trans.Ind.Electron.,55(4): 1715–1721

Yang CC, Hwang SJ, Lee HH, Huang DY (2007).Control of hot runner type micro injection molding module. Proc. IEEE IECON, pp. 2928-2933.

Zhang G (2000).Speed control of two-inertia system by PI/PID control. IEEE Trans. Ind. Electron., 47(3): 603-609.